Research Article **ISSN: 2349 – 7106**

Asian Journal of Research in Chemistry and Pharmaceutical Sciences

Journal home page: www.ajrcps.com

SYNTHESIS OF PURE AND MgCa CO-DOPED ZnO NANOPARTICLES AND THEIR STRUCTURAL, OPTICAL AND ANTIBACTERIAL PROPERTIES BY CO-PRECIPITATION METHOD

A. Jafar Ahamed*[1], M. Karthikeyan[1], P. Vijaya Kumar[2]

[1*]Post Graduate and Research Department of Chemistry, Jamal Mohamed College (Autonomous), Tiruchirappalli - 620 020, Tamil Nadu, India.
[2]Department of Chemistry, Asan College of Arts and Science - 639 003, Karur, Tamil Nadu, India.

ABSTRACT

The present study, undoped and MgCa co-doped ZnO NPs were successfully synthesized by chemical co-precipitation method without use of capping agent. The structural and morphological properties of pure and MgCa co-doped ZnO NPs were analyzed using X-Ray diffraction (XRD) studies, Field emission scanning electron microscopy (FESEM), Elemental analysis (EDAX), Fourier Transform Infrared Spectroscopy (FTIR) and optical properties was studied by UV–vis spectroscopy and Photoluminescence (PL) spectra. The antibacterial activity of pure and MgCa co-doped ZnO NPs have been investigated against *Escherichia coli* and *Staphylococcus aureus* bacterial strains. It has been interestingly observed that MgCa doping has enhanced the inhibitory activity of ZnO against *S. aureus* more efficiently than the *E. coli* bacterial strain.

KEYWORDS

Zinc Oxide, Nanoparticles, Optical properties, *S. aureus* and Antibacterial activity.

Author for Correspondence:

Jafar Ahamed A,
Department of Chemistry,
Jamal Mohamed College (Autonomous),
Tiruchirappalli, Tamil Nadu, India.

Email: agjafar@yahoo.co.in

INTRODUCTON

Metal oxide semiconductor nanomaterials have attracted attention due to their interesting properties and potential application in many important areas such as: microelectronics, sensing, environmental remediation, biomedicine etc. Generally, the properties of these materials are greatly affected by their size and shape[1,2], which generate interest in the synthesis of semiconductor nanoparticles exhibiting different shapes, such as nanobelts and nanowires[3,4], nanospheres[5], nanoplates[6] and nanoflowers[7], etc.

Zinc oxide (ZnO), an II–VI compound with wide direct band gap (3.37 eV) semiconductor has a table wurtzite structure. A large exciton binding energy of 60 meV and high electron mobility at room temperature makes it suitable for new application such as electro-photography, electro luminescence phosphorus, pigments in paints, flux in ceramic glazes, filter for rubber products, coatings for paper, sunscreens, medicines and cosmetics. Nanoparticles of ZnO have potential application in photocatalysis[8], ultraviolet (UV) light emitters[9,10], piezoelectric devices[11], photo luminescentdevice[12-14], photodetectors[15-18], photodiodes[19], and gas sensors[20,21]. There are many methods to synthesis nanomaterials other than by direct atom manipulation, chemical vapour deposition[22], solvothermal method[23], co-precipitation method[24], hydro thermal method[25], sol–gel method[26-29], vapour–liquid–solid method[30], solid-state reaction method[31] and so on. Among them, co-precipitation method has many advantages such as simple, inexpensive and having large area applications. In the present work, we report that undoped ZnO and MgCa co-doped ZnO NPs were synthesized by chemical co-precipitation method and their structural, optical and antibacterial properties have been investigated.

EXPERIMENTAL METHODS

Synthesis of pure ZnO nanoparticles

0.1 M $Zn(NO_3)_2.6H_2O$ solution was prepared by using double distilled water under constant stirring. While at room temperature, 0.8 M NaOH solution was added drop by drop. This solution was stirred constantly at a temperature of 80±5 °C for 4 hours. After completion of the reaction, the solution was allowed to settle for overnight and the supernatant liquid was discarded. The obtained white coloured precipitate was thoroughly washed with double distilled water to remove all the other ions and then centrifuged at 3000 rpm for 10 minutes. The final precipitate was dried in a hot air oven at 80 °C for 2 hours. The above resulting dried precursors was crushed into powder and calcined at 700 °C for 5 hours. The final product (ZnO) was stored in air tight container for further analysis.

Synthesis of MgCa co-doped ZnO nanoparticles

0.097 M $Zn(NO_3)_2.6H_2O$, 0.002 M $Mg(NO_3)_2.6H_2O$, 0.001 M $Ca(NO_3)_2.6H_2O$ solution and 0.8 M of NaOH were separately dissolved in each 100 ml of distilled water using four 200 ml beakers. At first, Zinc nitrate, Magnesium nitrate and Calcium nitrate solutions were mixed homogenously. Then, NaOH solution was added drop wise to the homogenous mixed solution which yields a white precipitate. The solution with the white precipitate was stirred at room temperature for 30 min, and then at temperature of 60 ^oC for 4 h. This solution was refluxed at room temperature for 24 h. Then, a clear solution was obtained, which found to be stable at ambient condition. Thereafter, the solution was washed several times with double distilled water and ethanol. Finally, the precipitate was dried at 120 °C. Thus, MgCa co-doped ZnO nanopowder was obtained. This sample was annealed at 700 ^oC for 5 hours.

Antibacterial Assay

The antibacterial activity of the undoped ZnO and MgCa co-doped NPs was studied against gram positive G+ (*Staphylococcus aureus*) and gram negative G- (*Escherichia coli*) bacterial strains using well diffusion method. Petri plates were prepared with 25 ml of sterile Muller Hinton agar (MHA, Himedia) and each bacterial pathogen was individually swabbed on MHA in separate plates. The antibacterial activity was tested at a concentration of 1.5 mg/ml with the required quantity of the NPs dispersed in dimethyl sulphoxide (DMSO). The zone of inhibition levels (mm) were measured after 24h and before this step, it was incubated overnight at 37°C. The standard antibiotic Amoxicillin was used as the positive control.

Characterization Studies

The phase purity of the synthesized NPs were determined by X-ray diffractometer (Model: X'PERT PRO PAN analytical). The morphological features of the sample were measured by Field emission scanning electron microscopy (Model: Carl Zess 55) with EDAX (ultras). The vibrational frequency was measured by Fourier transform infra-red spectroscopy (Perkin-Elemer). The absorption

spectrum of the sample was measured on Perkin-Elmer (Lambda 35). The PL emission study of the sample was carried out using Horiba Jobin YVON spectrofluorometer (model: FLUOROMAX-4, 450W high pressure Xenon lamp as the excitation source, photomultiplier at a range 325-550 nm).

RESULTS AND DISCUSSION

X-ray diffraction studies

The X-ray diffraction pattern for undoped ZnO and MgCa co-doped ZnO NPs are shown in Figure No.1. The XRD peaks are located at angles (2θ) of 31.732, 34.320 and 36.354, corresponding to the (100), (002) and (101) planes of the ZnO NPs, respectively. Similarly, other peaks found at angles (2θ) of 47.43, 56.49, 62.57, 66.27, 68.12, 69.04 and 76.99 correspond to the (102), (110), (103), (112), (201), (004) and (202) planes of the ZnO NPs, respectively. The standard diffraction peaks show that the hexagonal wurtzite structure of ZnO NPs with space group of p63mc. It is also confirmed by the JCPDS data (card No: 361451). It is also observed that there is no impurity phase found in the Mg^{2+} and Ca^{2+} co-doped ZnO sample, because of ionic radii of Mg^{2+} (0.66 Å) and Ca^{2+} (0.99 Å).

The average crystallite size of the ZnO NPs was estimated from X-ray line broadening of the diffraction peaks using Debye Scherrer's relation.

$$\text{Average crystallite size (D)} = \frac{0.9\,\lambda}{\beta \cos\theta} \quad \text{--- (1)}$$

Where D is the crystallite size, λ is the wavelength (1.5406 Å CuKα), θ is the Bragg diffraction angle and β is the full width at half maximum (FWHM). The average crystallite sizes of ZnO and MgCa co-doped ZnO nanomaterials were calculated to be 45 nm and 39 nm. Thus, the particle size decreases because of MgCa doping in ZnO nanostructures. This decrease in the crystallite size is due to distortion in the ZnO matrix by Mg^{2+}, Ca^{2+} dopant ions, which increases the rate of growth of ZnO.

Field Emission Scanning Electron Microscopy (FESEM) studies

The surface morphology of the undoped ZnO and MgCa co-doped ZnO NPs are shown in Figure No.2. From the FESEM images, the spherical and hexagonal like nanostructures were observed in undoped ZnO and MgCa co-doped ZnO NPs respectively. The average particle size were observed at 43 nm and 37 nm for ZnO and MgCa co-doped ZnO NPs respectively. The alkaline metal ions decreases the nucleation and subsequent growth rate of ZnO nanoparticles, so that the nanoparticles thickness is reduced.

Energy dispersive analysis of X-ray (EDAX) studies

The compositional analysis of the undoped ZnO and MgCa co-doped ZnO NPs were carried out using EDAX. The typical EDAX spectrum of the undoped ZnO and MgCa co-doped ZnO NPs are shown in Figure No.3. In the co-doped sample, MgCa composition is observed at 1.57 %. The chemical composition of Zn and O are found as 83.70 % and 16.30 % respectively. The EDAX spectra has indicated the presence of Zn, O, Mg, and Ca for the synthesized NPs. The obtained NPs are made up of only these elements, which shows that the Mg^{2+} and Ca^{2+} ions are substituting the Zn^{2+} ions in the ZnO matrix.

Fourier Transform Infrared (FTIR) studies

The FT-IR spectrum of the undoped ZnO and MgCa co-doped ZnO NPs are shown in Figure No.4. The synthesized undoped ZnO and MgCa co-doped ZnO NPs were analyzed by FT-IR in the range from 400 to 4000 cm^{-1} at room temperature. The FT-IR spectra contains several characteristic bands. A peak in the range of 3020-3650 cm^{-1}corresponds to the vibrational mode of O-H bond[32]. The Zn-O stretching band observed at 445 cm^{-1} for undoped ZnO NPs and in the case of MgCa co-doped ZnO NPs Zn-O stretching found to be 523 cm^{-1}. The peak around 1635 cm^{-1} is due to H−O−H bending vibration, which is assigned to a small amount of H_2O in ZnO NPs[33]. The asymmetric C-O stretching bands to be 1112 cm^{-1} and asymmetric C-H bands are observed at 2924 cm^{-1} for ZnO and MgCa co-doped ZnO NPs.

UV–Vis absorption spectroscopy

UV–visible optical absorption spectra were recorded at room temperature in the wavelength range 350–800 nm and shown in Figure No.5. The samples were uniformly dispersed in distilled water, followed by ultra sonification for 15–20 min before

recording UV–Vis spectra. From the absorption spectra, the absorption peaks are found at 377 nm for undoped ZnO NPs whereas the peaks are observed at 396 nm for MgCa co-doped ZnO NPs, which can be attributed to the photo excitation of electrons from valence band to conduction band[34].

Photoluminescence (PL) studies

The photoluminescence spectra of synthesized undoped ZnO and MgCa co-doped ZnO NPs recorded with the excited wavelength of 385 nm are shown in Figure No.6 (a-b). The PL emissions are observed for pure ZnO and MgCa co-doped ZnO NPs covering from the very short wavelength of 350 nm to long wavelength 600 nm. The recorded spectra fitted by Gaussian function with seven peaks for both ZnO NPs. The solid lines represent the linear combination of seven Gaussian peaks where 387 nm has the lowest and 516 nm has the highest wavelength. The emission spectra of the ZnO and MgCa co-doped ZnO NPs are having seven peaks at 387, 401, 416, 438, 457, 477, 516 nm and 389, 418, 436, 447, 481, 497, 524 nm respectively. These bands are violet emission,three blue emissions, blue-green emission, two green emissions respectively.

The UV emission peaks of lowest wavelength are observed at 387 and 389 nm, which correspond to the near-band emission (NBE) of ZnO NPs. The four violet emissions centered at 410, 411, 438 and 447 nm is ascribed to an electron transition from a shallow donor level of the natural zinc interstitials to the top level of the valence band[35]. The blue green emission observed at 477, 481 and 497 nm is ascribed to the transition between the oxygen vacancy and interstitial oxygen[36]. Finally two green emissions observed at 516 and 524 nm, corresponds to the singly ionized oxygen vacancies[37,38].

Antibacterial Activity

In the present work, the antibacterial activities of undoped ZnO and MgCa co-doped ZnO NPs are shown in Figure No.7. The antibacterial activities of synthesized undoped ZnO and MgCa co-doped ZnO NPs were tested against the human pathogens like Gram positive (*S.aureus*), and Gram negative (*E.coli*) bacteria with reference to Amoxicillin. The antibacterial activity values are listed in Table No.1. From the results, the zones were increased with respect to the MgCa co-dopant concentration against the tested bacteria. To compare the Gram positive and Gram negative bacteria, the observed inhibition zone was higher in gram positive bacteria which may be due to the difference in their cell wall structure of chemical composition. From these zone measurements, it could be stated that MgCa co-doped ZnO NPs have higher antibacterial property when compared to pure ZnO NPs. The antibacterial activity of NPs may either directly interact with the microbial cells or produce secondary products that cause damage[39].

Table No.1: Antibacterial activities of undoped ZnO and MgCa co-doped ZnO NPs for against human pathogens

S.No	Samples	*E.coli*	*S.aureus*
1	Undoped ZnO	1.3	1.7
2	MgCa co-doped ZnO	1.4	1.8
3	Std	0.8	1

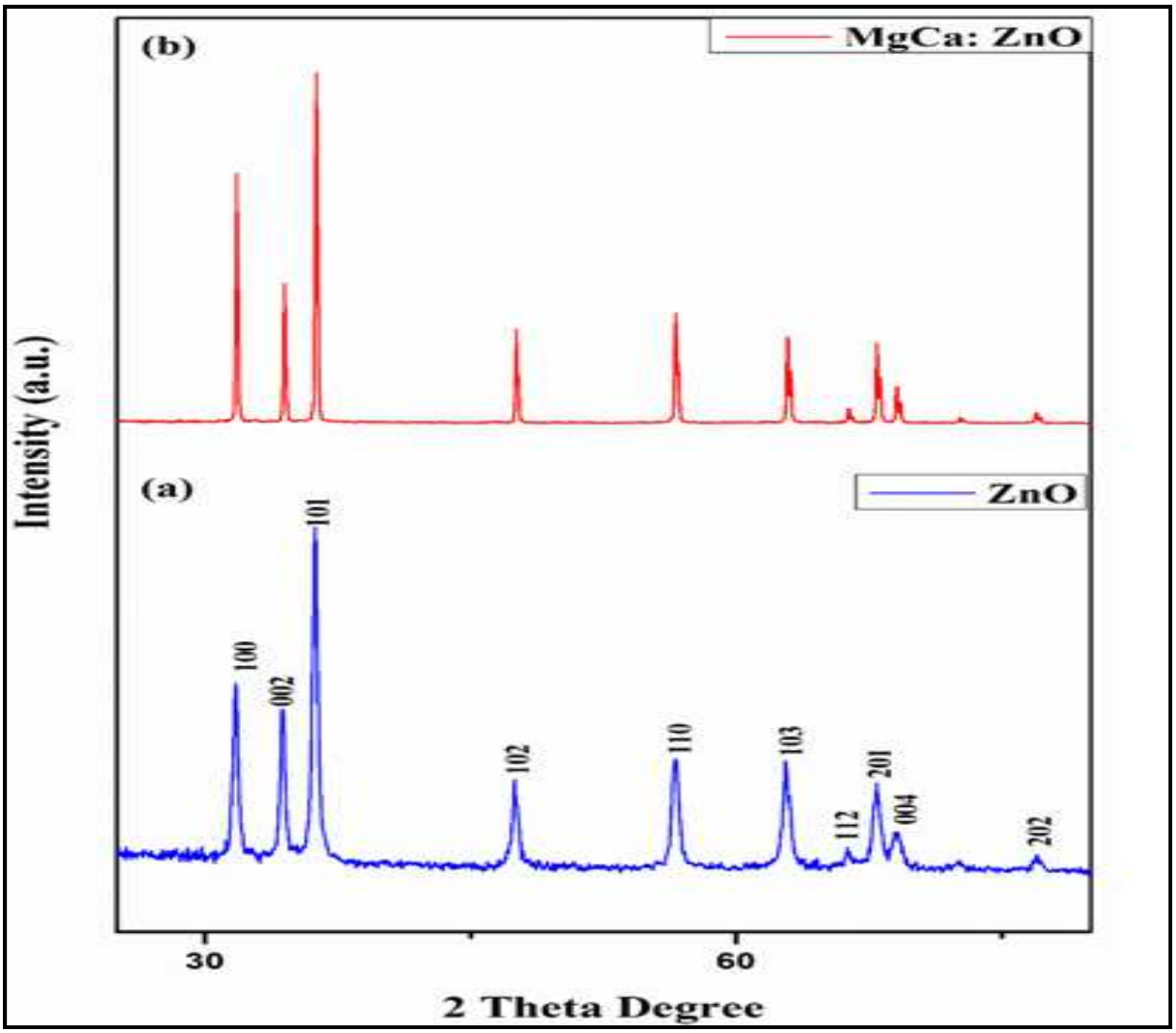

Figure No.1: XRD pattern of a) undoped ZnO and b) MgCa co-doped ZnO NPs

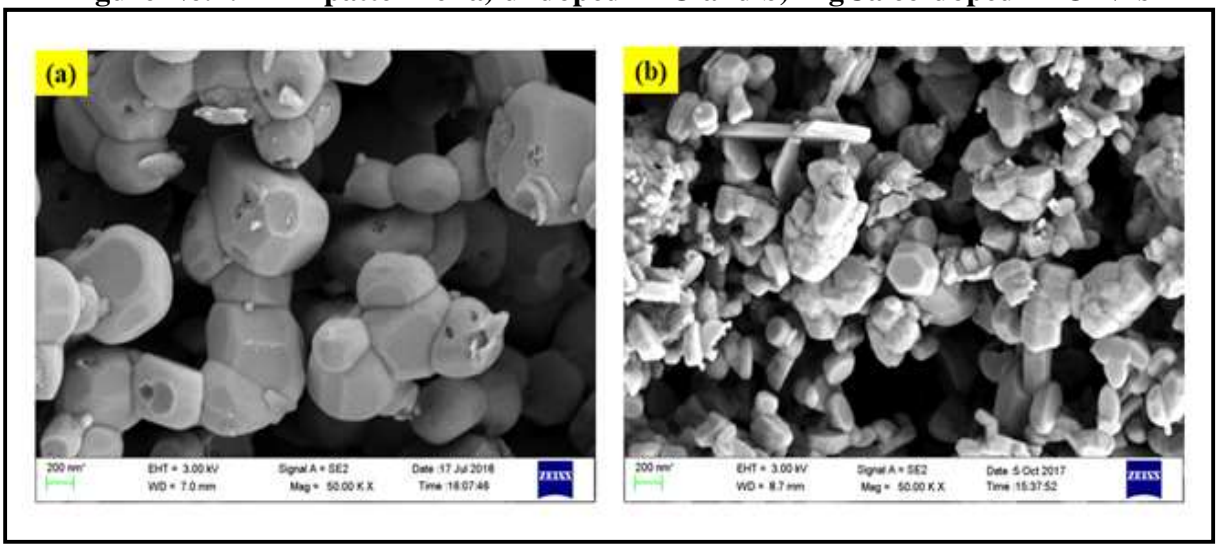

Figure No.2: FESEM images of a) undoped ZnO and b) MgCa co-doped ZnO NPs

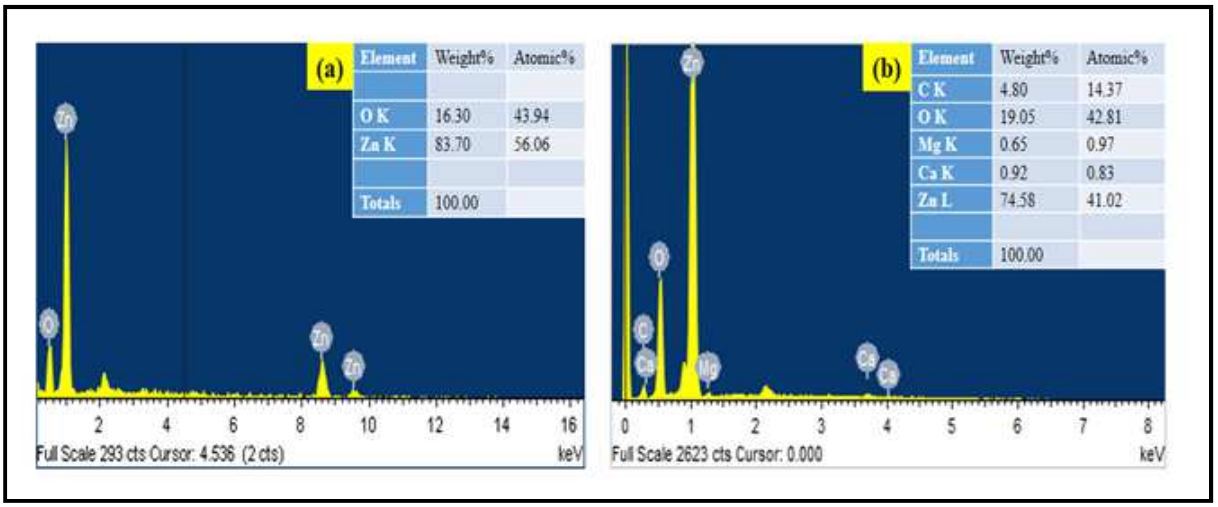

Figure No.3: EDAX spectra of a) undoped ZnO and b) MgCa co-doped ZnO NPs

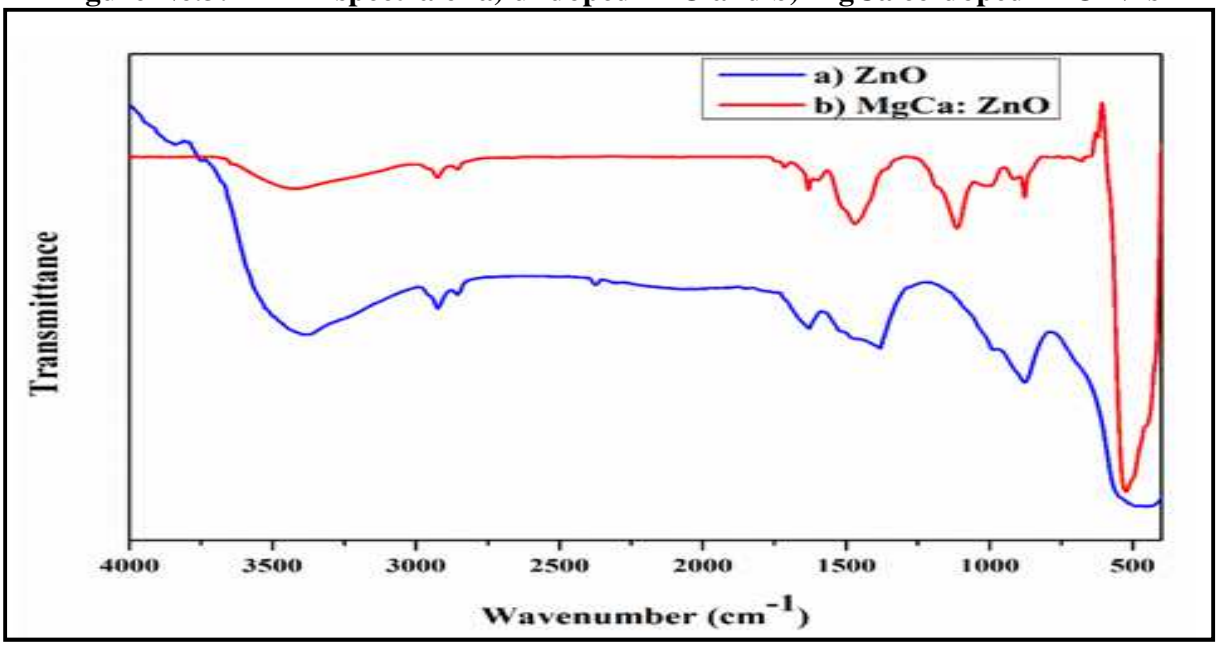

Figure No.4: FT-IR spectra of a) undoped ZnO and b) MgCa co-doped ZnO NPs

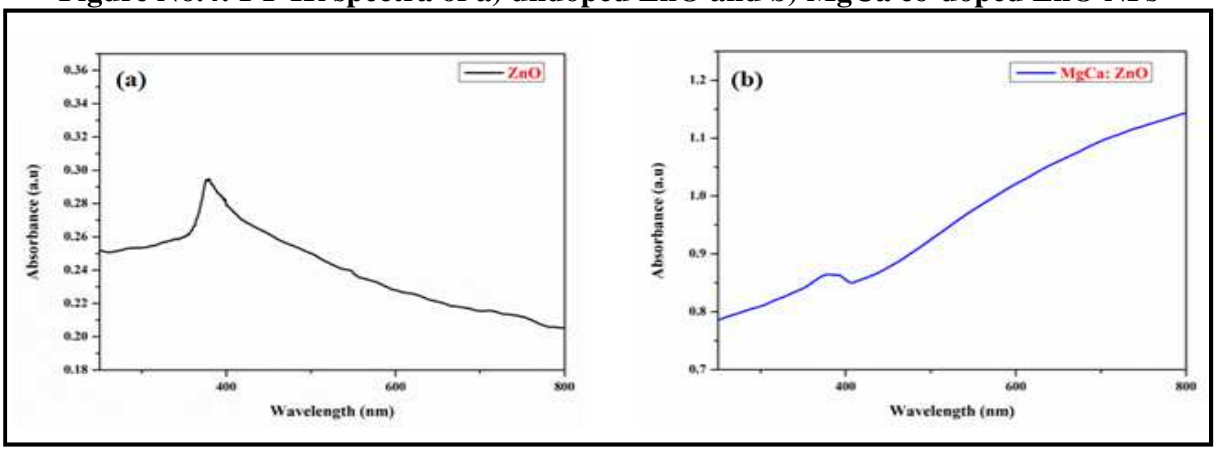

Figure No.5: Absorption spectra of a) undoped ZnO and b) MgCa co-doped ZnO NPs

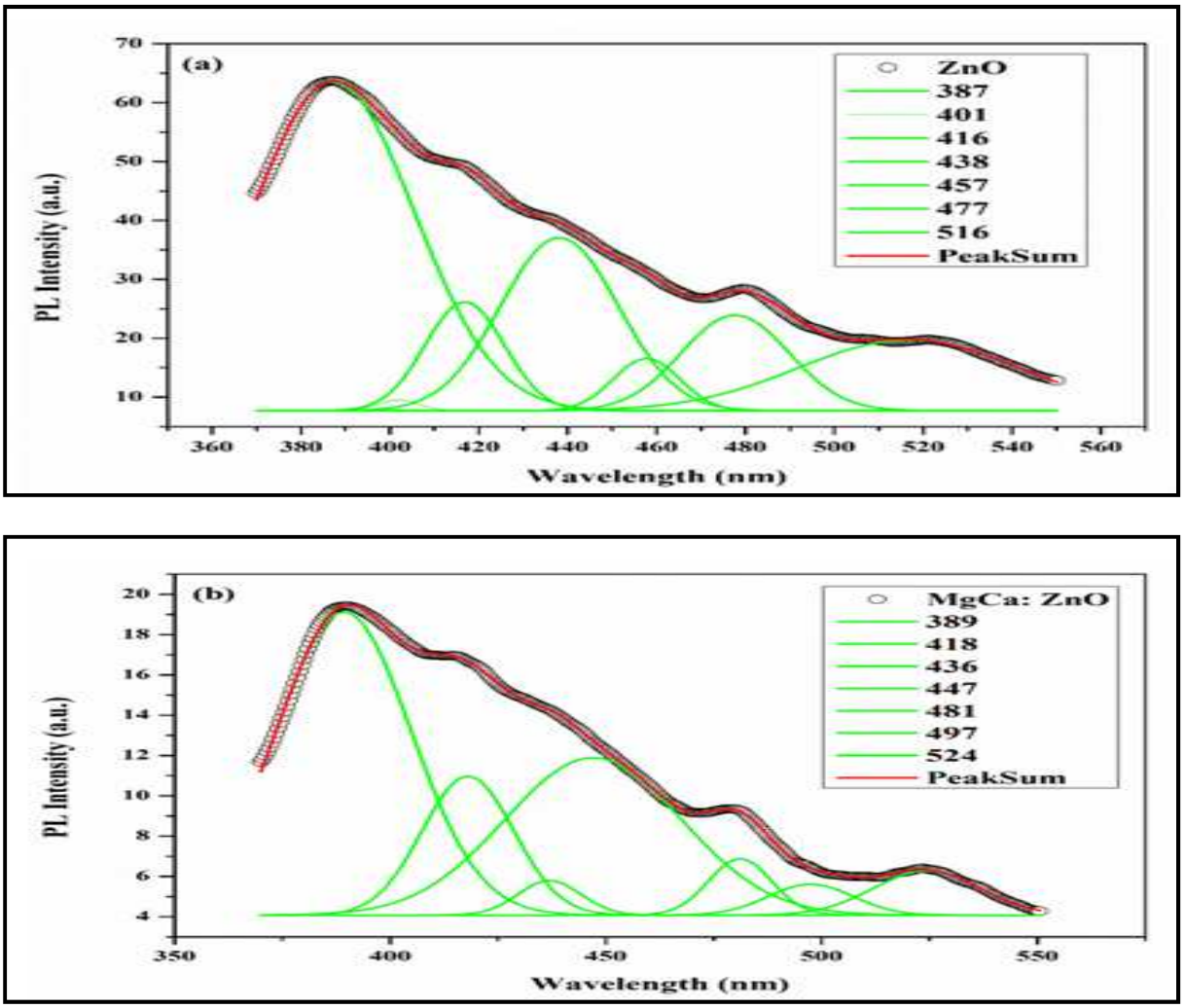

Figure No.6: (a) Gaussian de-composed photoluminescence emission spectra of undoped ZnO NPs : 6(b) Gaussian de-composed photoluminescence emission spectra of MgCa co-doped ZnO NPs

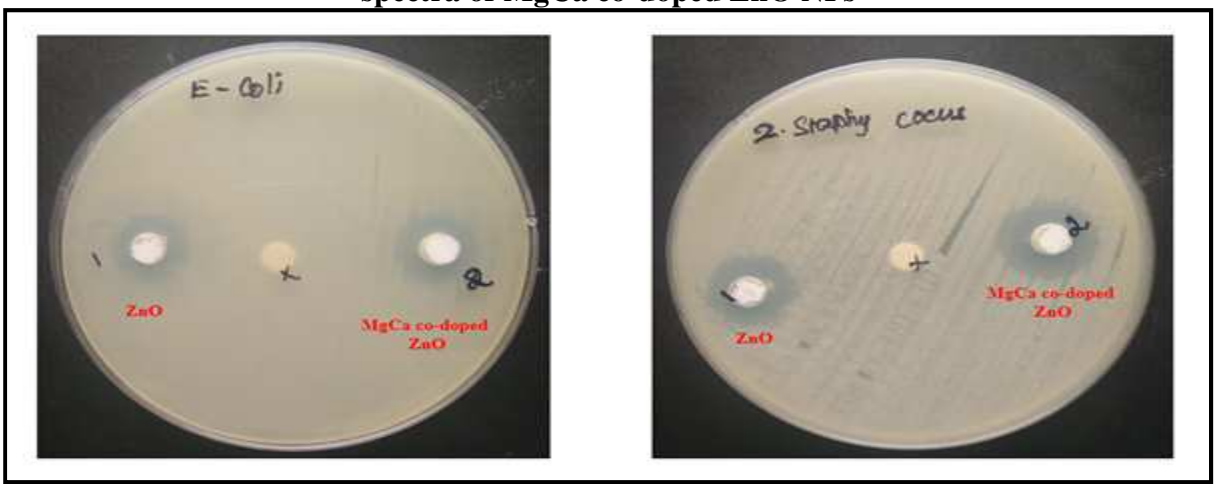

Figure No.7: Zone of inhibition of undoped ZnO and MgCa co-doped ZnO nanoparticles against *E. coli and S. aureus*

CONCLUSION

The undoped ZnO and MgCa co-doped ZnO NPs were prepared through co-precipitation method. The X-ray diffraction study confirmed that the prepared undoped ZnO and MgCa co-doped ZnO NPs have hexagonal wurtzite structure. The average particle sizes of undoped ZnO and MgCa co-doped ZnO NPs were 39 and 45 nm. The size of MgCa co-doped ZnO NPs are smaller when compared to pure ZnO NPs. This size reduction is mainly due to the distortion in the host ZnO lattice by the foreign impurities like Mg^{2+} and Ca^{2+} ions. From the FESEM images, the morphology of nanoparticles were found spherical and hexagonal in shape. The elemental composition was identified by EDAX spectra. From the FT-IR spectra, the Zn–O stretching frequency appeared at 445 cm^{-1} and 523 cm^{-1} for ZnO and MgCa co-doped ZnO samples. The UV-Vis spectrum showed the absorption peak is found at 377 and 396 nm for ZnO and MgCa co-doped ZnO NPs respectively. PL spectra showed that doping materials altered the band emission, which is due to zinc vacancy, oxygen vacancy and surface defects. The antibacterial studies performed against a set of bacterial strains showed that the MgCa co-doped ZnO NPs possessed more antibacterial property.

ACKNOWLEDGEMENT

The authors wish to express their sincere gratitude to Post Graduate and Research Department of Chemistry, Jamal Mohamed College (Autonomous), Tiruchirappalli - 620 020, Tamil Nadu, India for providing necessary facilities to carry out this research work.

CONFLICT OF INTEREST

We declare that we have no conflict of interest.

BIBLIOGRAPHY

1. Mclaren A, Valdes-Solis T, Li G, Tsang S C. Shape and size effects of ZnO nanocrystals on photocatalytic activity, *Journal of the American Chemical Society*, 131(35), 2009, 12540-12541.
2. Flores N M, Pal U, Galeazzia R, Sandoval A. Effects of morphology, surface area, and defect content on the photocatalytic dye degradation performance of ZnO nanostructures, *RSC Advances*, 4(77), 2014, 41099-41110.
3. Xi Y, Hu C G, Han X Y, Xiong Y F, Gao P X, Liu G B. Hydrothermal synthesis of ZnO nanobelts and gas sensitivity property, *Solid State Communications*, 141(9), 2007, 506-509.
4. Lu L, Chen J, Li L, Wang W. Direct synthesis of vertically aligned ZnO nanowires on FTO substrates using a CVD method and the improvement of photovoltaic performance, *Nanoscale Research Letters*, 7(293), 2012, 1-8.
5. Lin J H, Patil R A, Devan R S, Liu Z A, Wang Y P, Ho C H, Liou Y, Ma Y R. Photoluminescence mechanisms of metallic Zn nanospheres, semiconducting ZnO nanoballoons, and metal-semiconductor Zn/ZnO nanospheres, *Scientific Reports,* 4(6967), 2014, 1-7.
6. Zamirin R, Kaushal A, Rebelo A, Ferreira J M F. Er doped ZnO nanoplates: Synthesis, optical and dielectric properties, *Ceramics International*, 40(1), 2014, 1635-1639.
7. Xue X Y, Chen Z H, Xing L L, Ma C H, Chen Y J, Wang T H. Enhanced optical and sensing properties of one-step synthesized Pt−ZnO nano flowers, *Journal of Physical Chemistry C,* 114(43), 2010, 18607-18611.
8. Labhane P K, Huse V R, Patte L B, Chaudhari A L, Sonawani G H. Synthesis of Cu Doped ZnO nanoparticles: Crystallographic, Optical, FTIR, Morphological and Photocatalytic Study, *Journal of Materials Science and Chemical Engineering*, 3(9), 2015, 51.
9. Carrey J, Carrere H, Khan M L, Chaudret B, Marie X, Respaud M. Photoconductivity of self-assembled ZnO nanoparticles synthesized by organometallic chemistry, *Semiconductor Science and Technology*, 23(2), 2008, 025003.

10. Misra K P, Shukla RK, Srivastava A. Blue shift in optical band gap in nanocrystalline $Zn_{1-x}Ca_xO$ films deposited by sol-gel method, *Applied Physics Letters*, 95(3), 2009, 1901.
11. Carotta M C, Cervi A, Natale V D, Gherardi S, Giberti A, Guidi V, Puzzovio D. ZnO gas sensors: a comparison between nanoparticles, nanotetrapods-based thick films, *Sensors and Actuators B: Chemical,* 137(1), 2009, 164-169.
12. Oba F, Choi M, Togo A, Tanaka I. Point defects in ZnO: an approach from first principles, *Science and Technology of Advanced Materials*, 12(3), 2011, 4302.
13. Jiang M, Wang Z, Ning Z. Study of structural and optical properties of Ge doped ZnO films, *Thin Solid Films,* 517(24), 2009, 6717.
14. Udryabhaskar R, Mangalariaja R V, Karthikeyan B, Thermal annealing induced structural and optical properties of Ca doped ZnO nanoparticles, *Journal of Materials Science: Materials in Electronics,* 24(9), 2013, 3183-3188.
15. Rogach A L, Gaponik N, Lupton J M, Bertoni C, Gallardo D E, Dunn S, Pira N L, Paderi M, Repetto P, Romanov S G, O'Dwyer C, Torres C M S, Eychmüller A. Light-emitting diodes with semiconductor nanocrystals, *WILEY-VCH Verlag,* 47(35), 2008, 6538-6549.
16. Rogach A L, Eychmuller A, Hickey S G, Kershaw S V, Infrared-emitting colloidal nanocrystals: synthesis, assembly, spectroscopy, and applications, *Small,* 3(4), 2007, 536-557.
17. Konstantatos G, Howard I, Fischer A, Hoogland S, Clifford J, Klem E, Levina L, Sargent E H. Ultrasensitive solution-cast quantum dot photodetectors, *Nature,* 442(7099), 2006, 180-183.
18. Cho N, Roy Choudhury K, Thapa R B, Sahoo Y, Ohulchanskyy T, Cartwright A N, Lee K S, Prasad P N. Efficient Photodetection at IR Wavelengths by Incorporation of PbSe-Carbon U Nanotube Conjugates in a Polymeric Nanocomposite, *Advanced Materials,* 19(2), 2007, 232-236.
19. Lee J H, Chung Y W, Hon M H, Leu I C. Density-controlled growth and field emission property of aligned ZnO nanorod arrays, *Applied Physics A,* 97(2), 2009, 403-408.
20. Shalaka C, Navale A B, Mulla I S. Photoluminescence and Gas Sensing Study of Nanostructured Pure and Sn Doped ZnO, *Materials Science and Engineering C,* 29(4), 2009, 1317-1320.
21. Jiaqiang X, Yuping Xie C, Hu M, Gu Y, Bai Z, Zeng D. Structural characteristics and UV-light enhanced gas sensitivity of La-doped ZnO nanoparticles", *Materials Science and Engineering B,* 141(25), 2007, 43-48.
22. Purica M, Budianu E, Rusu E, Danila M, Gavrila R. 'Optical and Structural Investigation of ZnO Thin Films Prepared by Chemical Vapor Deposition (CVD), *Thin Solid Films,* 403-404, 2002, 485-488.
23. Madhu K U, Freeda T H, Mahadevan C K. Optical Properties of ZnO–CdS Nano Composite, *International Journal of Material Science,* 4, 2009, 549.
24. Rodriguezpaez J E, Caballero A C, Villegas M, Moure C, Duran P, Fernandez J F. Controlled Precipitation Methods: Formation Mechanism of ZnO Nanoparticles, Journal of the European Ceramic Society, 21(7), 2001, 925.
25. Aneesh P M., Vanaja K A, Jayaraj M K. Synthesis of ZnO nanoparticles by hydrothermal method, *Nanophotonic Materials, IV,* 6639, 2007, 0J(1-9).
26. Omri K, El Ghoul J, Lemine O M, Bouondina M, Zhang B, Mir L E. Magnetic and optical properties of manganese doped ZnO nanoparticles synthesized by sol–gel technique, *Superlattices and Microstructures,* 60, 2013, 139-147.
27. Caglar M, Yakuphanoglu F. Structural and optical properties of copper doped ZnO

films derived by sol-gel, *Applied Surface Science,* 258(7), 2012, 3039.
28. Rani S, Suri P, Shishodia P K, Mehra R M. Synthesis of Nanocrystalline ZnO Powder via Sol-Gel Route for Dye-Sensitized Solar Cells, *Solar Energy Materials and Solar Cells,* 92(12), 2008, 1639-1645.
29. Jacob S A, Rinu J E, Jaculine M M, Daisy A H, Das S J. Studies on sol gel synthesized Lanthanum doped gamma Manganese dioxide Nano rods, *International Journal of Chem Tech Research*, 6(3), 2014, 2135-2137.
30. Zhu Y, Zhou Y. Preparation of pure ZnO nanoparticles by a simple solid-state reaction method, *Applied Physics A*, 92, 2008, 275.
31. Gu F, Wang S F, Lu M K, Zhou G J, Xu D, Yuan D R. Structure Evaluation and Highly Enhanced Luminescence of Dy^{3+}-Doped ZnO Nanocrystals by Li^{+} Doping via Combustion Method, *Langmuir,* 20(9), 2004, 3528-3531.
32. Zandi S, Kameli P, Salamati H, Ahmad H, Hakimi M. Microstructure and optical properties of ZnO nanoparticles prepared by a simple method, *Physica B.,* 406(17), 2011, 3215-3218.
33. Sonawane Y S, Kanade K G, Kale B B, Aiyer R. C. Electrical and gas sensing properties of self-aligned copper-doped zinc oxide nanoparticles, *Materials Research Bulletin,* 43(10), 2008, 2719-2726.
34. Liu M, Kitai A H, Mascher P. Point defects and luminescence centres in zinc oxide and zinc oxide doped with manganese, *Journal of Luminescence,* 54(1), 1992, 35-42.
35. Fan X M, Lian J S, Zhao L, Liu Y. Single violet luminescence emitted from ZnO films obtained by oxidation of Zn film on quartz glass, *Applied Surface Science*, 252(2), 2005, 420-424.
36. Varghese N, Panchakarla L S, Hanapi M, Govindaraj A, Rao C N R. Solvothermal synthesis of nanorods of ZnO, N-doped ZnO and CdO, *Materials Research. Bulletin,* 42(12), 2007, 2117-2124.
37. Kumar N, Dorfman A, Hahm J. Fabrication of optically enhanced ZnO nanorods and microrods using novel biocatalysts, *Journal of Nanoscience and Nanotechnology*, 5(11), 2005, 1915-1918.
38. Bagnall D M, Chen Y F, Shen M Y, Zhu Z, Goto T and Yao T. Room temperature excitonic stimulated emission from zinc oxide epilayers grown by plasma-assisted MBE, *Journal of crystal growth,* 184-185, 1998, 605-609.
39. Karthikeyan M, Jafar Ahamed A, Vijayakumar P, Karthikeyan C. Green synthesis of pure ZnO and La doped ZnO nanoparticles and their structural, optical and antibacterial studies, *European Journal of Biomedical and Pharmaceutical Sciences,* 5(2), 2018, 736-741.

Please cite this article in press as: Jafar Ahamed A *et al.* Synthesis of pure and MgCa co-doped ZnO nanoparticles and their structural, optical and antibacterial properties by co-precipitation method, *Asian Journal of Research in Chemistry and Pharmaceutical Sciences,* 7(1), 2019, 167-176.